

Comparison of the interactions of H_2 and rare-gas atoms with surfaces of insulators

Majid Karimi

Department of Physics, Utica College, Utica, New York 13502

Gianfranco Vidali

Department of Physics, Syracuse University, Syracuse, New York 13244-1130

(Received 13 July 1988)

Calculations are presented for the interactions of H_2 , He, Ne, and Ar with the (001) surfaces of LiF, NaCl, and MgO. We have used a model potential that we developed previously and here applied to new systems. The proposed interaction potential has only one free parameter. This is chosen to be a coefficient describing the long-range interaction, since such a coefficient is the least well known. We then discuss the applicability of this model by comparing the results for different systems. In particular we discuss the He/MgO(001) system for which contradictory experimental determinations of the well depth exist.

I. INTRODUCTION

Considerable attention has been given recently to the study of the atom-surface interaction. There exists now a large body of experimental data on light atoms and molecules interacting with surfaces of metals and insulators.^{1,2} Most of the data come from atom-beam scattering (ABS) experiments. Calorimetric and neutron-scattering experiments have also yielded important information on the interaction.²

Various approaches have been used to study the atom-surface interaction from a theoretical standpoint. Because of the difficulties in modeling quantum mechanically a collision process that is strong and involves many particles, most of the theoretical efforts were dedicated to the construction of semi-empirical interaction potentials which would fit the experimental data.³⁻⁹

Recently, some interest has arisen in developing a theoretical framework aimed at interpretation of ABS data as due to the surface electron density. The question that has been debated is whether ABS can be used to obtain surface structural information.¹⁰ In order to use ABS, one has to know how sensitive the technique is in probing small changes of the surface electronic structures, such changes being produced, for example, by the presence of an adsorbate or by the reconstruction of the surface. To answer this question, one needs to have a good theoretical grasp of the atom-surface interaction. While there are still many important questions which are left unanswered, we think that we are starting to understand how to proceed towards this goal.

One method used to obtain this link between surface structure and ABS data, is to use the so-called effective-medium theory (EMT). While we refer the reader to good recent in-depth reviews on the subject,¹¹⁻¹³ here we can succinctly recall the essence of the EMT approach. Using density-functional methods in the local-density approximation, EMT calculates the cost in energy of embedding an atom in a homogeneous sea of electrons. The repulsive part of the atom-surface potential is then

written in terms of the surface electronic density *sampled* by the incoming atom (usually of 10 to 70 meV of energy). By measuring the scattering pattern in an ABS experiment, one should be able, using EMT, to deduce the surface electronic density, a quantity that usually cannot be measured by other experimental methods for such low densities, 10^{-4} electron/Å³. EMT-based approaches have been used mostly to study the scattering of helium atoms from metal surfaces¹⁰⁻¹³ and encouraging results were obtained. EMT could be applied, in principle, to other systems as well, such as He and other rare-gas atoms interacting with the surfaces of insulators. In fact, at the distances sampled by the incoming He atom, and as far as the surface electronic densities are concerned, the surface of an insulator looks similar to the one of a metal. The most important difference is the decay constant of the charge density extending into the vacuum. The question arises of whether this procedure can be extended to other systems. Preliminary calculations have been done for a few systems⁶⁻⁹ with various degrees of success. We address in this paper the issue of evaluating the strengths and weaknesses of the EMT approach by comparing the interaction of light and heavy rare-gas atoms plus molecular hydrogen with the (001) surfaces of LiF, NaCl, and MgO.

In the subsequent sections we present a model of the atom-surface potential based on semi *ab initio* calculations of the attractive and repulsive parts of the interactions. Our model has evolved from the work in Refs. 6-9; the purpose of this paper is to point out the critical parameters that enter in the model. To do so, we compare the results obtained for the various systems in order to extract the major trends of the proposed model. We think that such comparison is useful to identify major trends and to initiate new calculations or experiments.

II. THE MODEL

The basic approach to calculate the potential has been described in detail in Refs. 6-9; Here we present the

highlights of the model as applied to the systems of interest. The interaction may be written as

$$V(\mathbf{r}) = V_A(\mathbf{r}) + V_R(\mathbf{r}) + V^{\text{in}}(\mathbf{r}), \quad (1)$$

V_A is the attractive part, V_R the repulsive one, and V^{in} represents the potential due to the surface electric field. Using damped dipole ($C_6^\pm f_6^\pm / r^6$) and damped quadrupole ($C_8^\pm f_8^\pm / r^8$) terms for the pair potential one can evaluate the lateral average and higher Fourier coefficients of V_A as^{3,9}

$$V_{0A}(Z) = \frac{2\pi}{a^2} [-(C_6^+ + C_6^-) \xi(4, Z/d)/4d^4 - (C_8^+ + C_8^-) \xi(6, Z/d)/6d^6 + H_0^+(Z) + H_0^-(Z)], \quad (2a)$$

$$V_{GA}(Z) = \frac{2\pi}{a^2} \sum_l (-1)^{l(m_1+m_2)+1} \times \left[[C_6^+ + (-1)^{m_1+m_2} C_6^-] \frac{1}{2!} \left[\frac{G}{2Z} \right]^2 \times K_2(GZ) + [C_8^+ + (-1)^{m_1+m_2} C_8^-] \times \frac{1}{3!} \left[\frac{G}{2Z} \right]^3 K_3(GZ) + H_G^+(Z) + H_G^-(Z) \right], \quad (2b)$$

$$H_G^+(Z) = \int_0^\infty J_0(GR) [C_6^+ (1 - f_6^+)/r^6 + C_8^+ (1 - f_8^+)/r^8] R dR, \quad (2c)$$

$$f_{2n}^+(r) = 1 - \sum_{k=0}^{2n} (\gamma_+ r)^k / k! e^{-\gamma_+ r}, \quad (2d)$$

where a is the lattice constant, $\xi(n, x)$ is the Riemann zeta function,⁷ $d = a/\sqrt{2}$ is the interlayer distance, C_6^+, C_8^+ and C_6^-, C_8^- are dispersion coefficients of the interactions between the incoming atom and the positive and negative ions in the solid, K_2 and K_3 are the modified Bessel functions, $\mathbf{G} = (2\pi/a)(m_1, m_2)$ is the reciprocal lattice vector, $\mathbf{r} = (\mathbf{R}, Z)$ is the vector from the adsorbate to the ions in the crystal, J_0 is the Bessel function, and γ_i is the decay constant of the charge densities of the ions of the surface. Similar formula can be found for $H_G^-(z)$ by replacing the + superscript with the -. $H_0^\pm(z)$ has been evaluated analytically (7).

The repulsive part $V_R(\mathbf{r})$ of the atom-surface interaction is related to the average of the charge density of the surface using EMT,

$$V_R(\mathbf{r}) = \alpha_{\text{eff}} \bar{\rho}(\mathbf{r}) + \Delta E_{\text{cov}}, \quad (3a)$$

$$\alpha_{\text{eff}} = \alpha_0 - \alpha_{\text{at}}, \quad (3b)$$

$$\alpha_{\text{at}} = \int \varphi_a(\mathbf{r}' - \mathbf{r}) d\mathbf{r}', \quad (3c)$$

$$\bar{\rho}(\mathbf{r}) = \frac{1}{\alpha_{\text{at}}} \int_{\Omega} \rho(\mathbf{r}') \varphi_a(\mathbf{r}' - \mathbf{r}) d\mathbf{r}'. \quad (3d)$$

All the integrals are performed over a sphere of volume

Ω and radius R_C . The rest of these quantities have been already defined in Refs. 6–9. ΔE_{cov} represents the energy contribution from hybridization of adatom and host energy levels. For He and closed shell systems this term is small. We will ignore it. For an ionic crystal we can write

$$V_{0R} = \alpha_{\text{eff}} (\bar{\rho}_0^+ + \bar{\rho}_0^-), \quad (4a)$$

$$V_{GR} = \alpha_{\text{eff}} (\bar{\rho}_G^+ + \bar{\rho}_G^-), \quad (4b)$$

where α_{eff} is derived in the Appendix. $\bar{\rho}_G^+$ and $\bar{\rho}_G^-$ can be evaluated analytically for $r > R_c$ if the charge densities of the ions on the surface can be approximated by simple exponentials (results are presented in the Appendix). The choice of R_c is discussed in Ref. 11. For other systems considered here, we found that for a given r , V_R is approximately independent of R_c for $2 < R_c < 3$ Å. For other values of R_c , V_R is smaller, in accordance to what was found in Ref. 11. We decided to take $R_c = 2.5$ Å for all systems.

The third term in Eq. (1) is the induced dipole energy due to the polarization of the adatom in the field of the lattice. This has been evaluated many times in the literature (3). The lateral average and higher Fourier coefficients $V_{m_1 m_2}$ are

$$V_{00}^{\text{ind}}(Z) = -\alpha \left[\frac{8\pi e}{a^2 [1 + \exp(-\sqrt{2}\pi)]} \right]^2 \exp(-4\pi Z/a), \quad (5a)$$

$$V_{11}^{\text{ind}}(Z) = \frac{1}{4} V_{00}^{\text{ind}}(Z). \quad (5b)$$

Once the atom-surface potential is constructed, a comparison to experimental data can be made. This will be done in Sec. III.

Of interest is also the study of the interaction between an atom and an adsorbate plated surface. Below we give an expression for the long-range part of the interaction for the systems mentioned above. In a future work we will present the complete atom-overlayer plus surface interaction. The long-range interaction between an atom and a substrate plated with one or more layers of adatoms can be written^{14–18} as

$$V(Z) = -\frac{C_3}{(Z+d)^3} - \frac{n_f \pi d_1}{2z^4} (C_6^{\text{ap}} + C_{S_2}), \quad (6a)$$

$$C_3 = \frac{1}{4\pi} \int_0^\infty dE g(iE) \alpha_a(iE), \quad (6b)$$

$$C_6^{\text{ap}} = \frac{3}{\pi} \int_0^\infty dE \alpha_a(iE) \alpha_p(iE), \quad (6c)$$

$$C_{s_1} = \frac{3}{\pi} \int_0^\infty dE \alpha_a(iE) \alpha_p(iE) g(iE), \quad (6d)$$

$$C_{s_2} = \frac{3}{\pi} \int_0^\infty dE \alpha_a(iE) \alpha_p(iE) [g(iE)]^2, \quad (6e)$$

where n_f and d_1 are the density and thickness of the overlayer film, respectively. Using the well-tested approximations for g , α_a , and α_p ,^{15–18} we obtain

$$C_3 = \frac{\alpha_{0a} g_0}{8} \frac{E_a E_s}{E_a + E_s}, \quad (7a)$$

$$C_6^{ap} = \frac{3}{2} \alpha_{0a} \alpha_{0p} \frac{E_a E_p}{E_a + E_p}, \quad (7b)$$

$$C_{s_1} = \frac{3g_0 \alpha_{0a} \alpha_{0p} E_s y_a y_p (1 + y_a + y_p)}{2(1 + y_a)(1 + y_p)(y_a + y_p)}, \quad (7c)$$

$$C_{s_2} = \left[\frac{g_0 C_{s_1}}{2} \right] \left[2 + y_a + y_p + \frac{y_a}{1 + y_p} + \frac{y_p}{1 + y_a} \right] / (1 + y_a + y_p), \quad (7d)$$

$$y_i = E_i / E_s. \quad (7e)$$

All of the parameters in the above formulas are defined in Refs. 15–18.

III. RESULTS

In Table I we are reporting the results of interaction potentials for the systems of interest. We have inserted $v_0(z)$ for each system in the Schrödinger equation and evaluated the eigenvalues and position expectation values. In Table I these values are compared with the experimental results of Refs. 5 and 25–28. To obtain the best agreement we decided to use C_6^- as free parameter. The parameter q in the table gives the amount by which C_6^- should be multiplied (see also Sec. IV). There is some evidence to believe that data of Ref. 28 for He-MgO might be wrong. Although these data were previously used to construct a potential for He-MgO,⁸ we decided to use the new data²¹ to build a potential for the same system. Our values of $q = (C_6^-)_{\text{fit}} / (C_6^-)_{\text{theor}} = 1, 1.07$ for SMV and MJF data compared to the previous value of 1.68 provides some validity for the data of Ref. 27 (see also the discussion in Sec. IV). From the experimental point of view further work is needed to produce reliable and accurate data for He-MgO.²⁷ From the theoretical point of view a close-coupling calculation could be useful to assess the validity of the present data. We are in the process of setting up such calculations. When no adjust-

TABLE I. Comparison between the experimental and theoretical predictions of mean distance $\langle z \rangle$, well depth D , corrugation ξ at $V = 10$ meV, fitting parameter q , and energy level E_n with the calculations of the paper. Energies are in meV; lengths are in Å. [] are experimental values from Refs. 25 and 26. { } are experimental values from Refs. 27 and 24.

System	$\langle z \rangle$	D	ξ	q	$-E_0$	$-E_1$	$-E_2$	$-E_3$
H ₂ -LiF	3.36	(23.6) ^b (14.23) ^a	0.50 (0.4) ^b	1.45	17.26	8.39	3.59	1.32
H ₂ -NaCl	3.43	(37.31) ^b (18.3) ^a	1.0	1.68	29.48	17.42	9.49	0.82
H ₂ -MgO	3.35	33.00 (18.22) ^a	0.30	1.51	(26.28)	15.83	8.84	0.88
He-LiF	3.26	8.70 (7.03) ^a	0.61 (0.52) ^a	1.17 1	5.91 (4.58) ^a [5.90]	2.40 (1.66) ^a [2.46]	0.80 (0.48) ^a [0.78]	0.20 (0.08) ^a [0.21]
He-NaCl	3.76	(8.72) ^b 6.19 (7.91)	(0.52) ^b 1.20 (1.05) ^a	0.82 1	(5.92) ^b 4.07 (5.49) ^a [4.1]	(2.44) ^b 1.51 (2.32) ^a [1.5]	(0.84) ^b 0.45 (0.22) ^a [0.31]	(0.22) ^b ()
He-MgO	3.77	7.85 (6.90) ^a	0.42 (0.47) ^a	1.07 1	5.41 (4.85) ^a {4.82} {5.32}	2.49 (2.15) ^a {2.62}	1.00 (0.81) ^a {1.17}	0.33 (0.25) ^a {0.49}
Ne-LiF	3.02	(13.3) ^b (19.06) ^a	0.55 (0.59) ^b	0.77	11.66	6.44	3.24	1.46
Ne-NaCl	3.26	(18.40) ^b (20.8) ^a	1.20	0.91	16.53	13.21	10.41	6.16
Ne-MgO	3.44	(23.4) ^b (17.3) ^a	0.50	1.24	18.09	15.04	10.10	6.51
Ar-LiF	2.80	(77.0) ^b (54.65) ^a	0.50 (0.28) ^b	1.28	74.62	68.82	63.34	58.17
Ar-NaCl	3.11	(76.1) ^b (66.4) ^a	1.15	1.10	73.32	69.97	62.90	58.08
Ar-MgO	3.22	(74.5) ^b (59.2) ^a	0.48	1.18	72.03	67.29	62.76	58.44

^aPredictions of our model with no adjustable parameter i.e., $q = 1$.

^bPredictions of other models (Refs. 3, 4, 5, 25, and 19–23).

able parameter, i.e., $q=1$, is used, good agreement with experimental data is obtained; this provides some support for the validity of the present model. We should also mention that the most reliable determination of adsorption energies come from ABS experiments. These experiments were done for He-LiF, NaCl, and MgO only. We calculated the corrugations of the atom-surface potential across the surface for each system as it is seen by the incoming atoms. The maximum variation of the distance of closest approach to the surface by a 10-meV atom incident along the direction of unlike atoms ("corrugation") is reported in Table I. The calculated corrugations differ from the values obtained using a hard-wall model. This is partly due to the use of EMT which was observed to overestimate the corrugation^{9,10,13} and inadequacy of the hard-wall model in describing highly corrugated surfaces. In the case of NaCl, the larger corrugation, as compared with LiF and MgO, can be attributed to the larger lattice constant of NaCl. In parentheses we report

the results of our calculation with no adjustable parameter. Because of the uncertainty in the determination of C_6^- coefficient we decided to consider it as the only free parameter. (C_6^+ has a minor role in determining potential Ref. 9.) The value of q gives the factor that should be multiplied by C_6^- to obtain the best fit to available data, which are either bound state resonances or well depths of the laterally averaged potential, see Table I.

In Table II we report the result of our calculation for C_3 , C_6^{ap} , C_{s_1} , and C_{s_2} . The long-range interaction between an atom and a rare-gas plated surface is one of the building blocks to construct a potential between an incoming atom and an overlayer of rare gas atoms on the substrate. Such systems have received considerable attention by many experimental groups.

It has been shown in Ref. 29 that bound-state energies, when scaled appropriately, will all lie approximately on the same curve $J(\epsilon_n)$ reported in Ref. 29. Levels were

TABLE II. Input parameters for the long-range interaction between the adsorbates H, H₂, He, and rare-gas plated LiF, NaCl, and MgO surfaces. All lengths are in Å and energies are in meV.

Adsorbate	Plate	Substrate	C_3^a	C_6^{apb}	$C_{s_1}^b$	$C_{s_2}^b$
H	Ne	LiF	0.192	3.392	0.817	0.219
H	Ar	X	0.192	11.818	3.039	0.841
H	Kr	X	0.192	16.969	4.437	1.239
H	Xe	X	0.192	25.759	6.849	1.929
H ₂	Ne	X	0.274	4.717	1.090	0.287
H ₂	Ar	X	0.274	16.048	4.003	1.089
H ₂	Kr	X	0.274	22.888	5.822	1.600
H ₂	Xe	X	0.274	34.505	8.947	2.484
He	Ne	X	0.092	1.822	0.359	0.088
He	Ar	X	0.092	5.675	1.262	0.325
He	Kr	X	0.092	7.907	1.812	0.473
He	Xe	X	0.092	11.644	2.748	0.729
H	Ne	NaCl	0.219	3.392	1.009	0.346
H	Ar	X	0.219	11.818	3.786	1.338
H	Kr	X	0.219	16.969	5.543	1.978
H	Xe	X	0.219	25.760	8.581	3.092
H ₂	Ne	X	0.291	4.717	1.337	0.448
H ₂	Ar	X	0.291	16.048	4.961	1.721
H ₂	Kr	X	0.291	22.888	7.236	2.539
H ₂	Xe	X	0.291	34.505	11.157	3.957
He	Ne	X	0.097	1.822	0.431	0.134
He	Ar	X	0.097	5.675	1.538	0.503
He	Kr	X	0.097	7.907	2.218	0.737
He	Xe	X	0.097	11.644	3.379	1.141
H	Ne	MgO	0.290	3.392	1.193	0.470
H	Ar	X	0.290	11.818	4.443	1.802
H	Kr	X	0.290	16.969	6.490	2.655
H	Xe	X	0.290	25.760	10.020	4.136
H ₂	Ne	X	0.394	4.717	1.592	0.613
H ₂	Ar	X	0.394	16.048	5.851	2.332
H ₂	Kr	X	0.394	22.888	8.511	3.427
H ₂	Xe	X	0.394	34.505	13.803	5.324
He	Ne	X	0.142	1.822	0.523	0.187
He	Ar	X	0.142	5.675	1.842	0.694
He	Kr	X	0.142	7.907	2.646	1.012
He	Xe	X	0.142	11.644	4.014	1.560

^a C_3 in units of eV Å³; parameters in C_3 are from Refs. 15–17.

^b C_6^{ap} , C_{s_1} , C_{s_2} are in units of eV Å⁶; parameters are from Refs. 15–17.

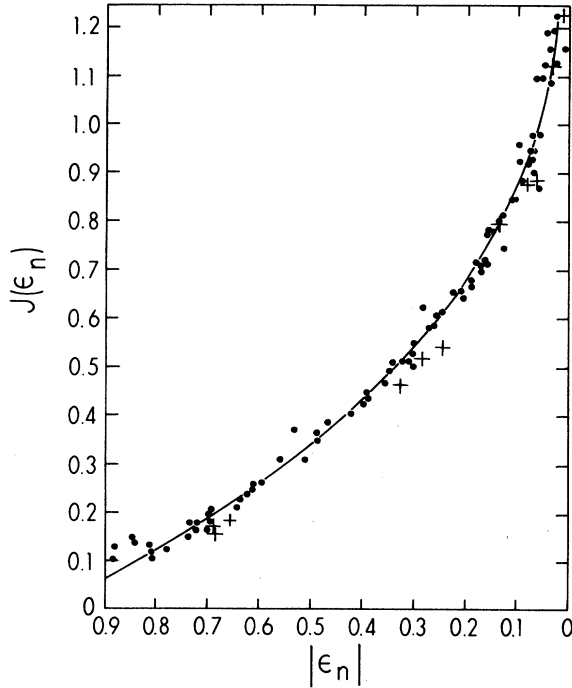


FIG. 1. Bound-state energy levels for systems listed in Ref. 23. The bound states for He-LiF, He-MgO, and He-NaCl are shown with + signs.

scaled as follows:

$$J(\epsilon_n) = (n + \frac{1}{2})b, \quad (8a)$$

$$b = \frac{4.542}{\sqrt{m} D^{0.166} C_3^{0.333}}, \quad (8b)$$

$$l_1 = (C_3/D)^{0.333}, \quad (8c)$$

$$\epsilon_n = E_n/D, \quad (8d)$$

n is an integer, b is a unitless quantity, m is the atomic mass unit of the adsorbate, D is the corrected well depth in meV, C_3 is in $\text{meV} \text{\AA}^3$, and l_1 is a characteristic length. In Fig. 1, on the original plot of Ref. 29, we have added the energy levels as determined from Eq. (8) and Table I for He-LiF, NaCl, and MgO. The agreement with the universal law curve is as good as for the other systems shown in Fig. 1 and discussed in Ref. 29.

IV. DISCUSSION

The calculations presented here are sensitive to three parameters: α_{eff} , the charge densities of the ions, and C_6^- coefficient. Below we comment on how these parameters were obtained and how reliable their determination is.

As far as the first point is concerned, α_{eff} is determined using Eq. (3b) through α_0 and α_{at} . α_0 has been calculated previously for the gas atoms and/or molecules of interest here.³⁰ α_{at} depends on the charge density of the atom. This formulation, Eqs. (3a)–(3d), initially developed for a “jellium” surface in the low surface-electron density limit, could be applied to other systems. Besides the limitations under which Eqs. (3) were derived, EMT uses essen-

tially a perturbation approach, there are some technical difficulties when Eqs. (3) are applied for electron densities appropriate of insulators. At these low densities and for rare-gas atoms, the difference between an insulator and a metal lies in the different gradients of the electron charge density protruding in vacuum. For a typical surface of an insulator such slope is larger than for the surface of a metal. The inhomogeneity of the charge density is taken into account to first order. Other terms might be necessary to correct for the larger gradient.

As for the second point, various methods have been followed to obtain the charge densities of the ions in the crystal. In general, in-crystal charge densities for most of the systems considered here are not available. Only for MgO the in-crystal charge densities of Mg^{2+} and O^{2-} were available.⁸ The use of free ion-charge densities leads to an overestimation of the corrugation and well depth.⁹ We have used the repulsive potentials of Refs. 3 and 4 to obtain the ion-charge densities using the following relation:

$$V_R = \alpha_{\text{eff}} \bar{\rho}.$$

While this procedure is obviously unsatisfactory from a formal standpoint, it should convey the physically correct idea that the repulsive part, no matter how it is calculated, should reflect the fact that it is due to the interaction of the incoming atom with the charge density of the solid. We remind the reader that the potentials of Refs. 3 and 4 fit remarkably well the copious ABS data on LiF and NaCl, see Table I. References 3 and 4(b) use a free parameter, as we do, to fit ABS data; Ref. 4(a) does not and its predictions differ from ABS data somewhat. Relaxation of the surface was not considered, though it could have some effect on the repulsive part of the potential.

Third, the uncertainty in C_6^- coefficient is estimated to be about 33% for He-LiF (Ref. 3) and, therefore, is the major source of concern here. This is why we decided to consider C_6^- as the free parameter. C_3 can be evaluated using $C_3 = n\pi/6(C_6^+ + C_6^-)$ (i.e., pairwise sum formula), where n is the number density of positive (or negative) ions in the solid ($n = \sqrt{2}/a^3$, where $a = 2.98 \text{\AA}$ for MgO). C_3 values 135, 122, and 212 $\text{meV} \text{\AA}^3$ computed using the pairwise sum, for He-LiF, NaCl, and MgO can be compared with 93, 106, and 128 $\text{meV} \text{\AA}^3$ obtained from the optical data (i.e., Lifshitz formula).^{15–18} The difference between the two sets of C_3 comes about because the Lifshitz approach takes into account dielectric screening, which is neglected in the pairwise sum, and because of the uncertainties in C_6^+ and C_6^- values.

Our values of $C_3 = 135$ and 122 $\text{meV} \text{\AA}^3$ for He-LiF and He-NaCl, respectively are in good agreement with the values of 137 and 121 $\text{meV} \text{\AA}^3$ obtained in Refs. 3 and 4.

The parameter q introduced in Sec. III was found to change little for rare gases on surfaces. On the other hand, such a correction is larger for H_2 . At this stage, we are unable to say whether this correction is due to: (1) uncertainties in determination of C_6^- values; (2) uncertainties in α_0 ; (3) inadequacy of Eqs. (3) to describe a more inhomogeneous system; or (4) poorly determined

experimental values. We remark that the corrugation is little affected by a change in C_6^- .

We may summarize our results as follows. The EMT, tested previously for He,Ne,Ar,H₂/graphite,^{6,7} He/LiF,⁹ He/NaCl,⁹ and He,Ar,Kr,Xe/MgO,⁸ provides a useful starting point for addressing the interactions of H₂, Ne, Ar/LiF, H₂, Ne, Ar/NaCl, and H₂,Ne/MgO. Our model predicts a smaller value of α_0 or D for the systems involving H₂. EMT can be extended to more systems provided that values of α_0 are known. More accurate values of α_0 , C_6^- , and in-crystal charge densities of ions are necessary. When C_6^- is allowed to be adjusted, a good agreement with experimental values is found.

ACKNOWLEDGMENTS

We thank Dr. Vilches and Dr. Frankl for communicating to us, prior to publication, data on H₂/MgO and He/MgO, respectively. We would like to acknowledge

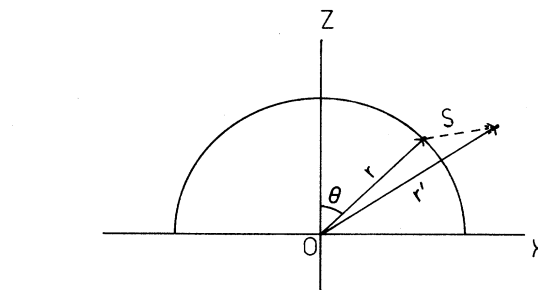


FIG. 2. The system of coordinants used to evaluate integrals in the Appendix.

support from the Alfred P. Sloan Foundation (G.V.), from the Research Corporation (New York, NY), and by the Donors of the Petroleum Research Fund, administered by the American Chemical Society.

APPENDIX

$$\begin{aligned} \alpha_{at} &= e \int_{\Omega} \varphi_a(\mathbf{r}' - \mathbf{r}) d\mathbf{r}' = e \int_{\Omega} \varphi_a(|\mathbf{S}|) d\mathbf{S} = 2\pi z_a e^2 \int_0^{R_c} \left[\beta e^{-\beta S} + \frac{2}{S} e^{-\beta S} + \beta^2 \left[R_c + \frac{1}{\beta} \right] e^{-\beta R_c} \right] S^2 dS \\ &= \frac{8\pi z_a e^2}{\beta^2} \left\{ 1 - \left[1 + R_c \beta + \frac{R_c^2 \beta^2}{4} - \frac{R_c^3 \beta^4}{12} \left[R_c + \frac{1}{\beta} \right] \right] \exp(-\beta R_c) \right\}, \quad (A1) \end{aligned}$$

where β is the decay constant of the charge density of the adsorbate, z_a is the effective atomic number of the adsorbant, and e is charge of an electron.

$$\begin{aligned} \overline{\rho}_G^+ &= \frac{e}{\alpha_{at}} \int_{\Omega} \sum_i \rho_i^+(\mathbf{r}') \varphi_a(\mathbf{r}' - \mathbf{r}) d\mathbf{r}' = \frac{e}{\alpha_{at}} \sum_i \int_{\Omega} \rho_i^+(|\mathbf{r} + \mathbf{S}|) \varphi_a(|\mathbf{S}|) d\mathbf{S}, \\ \overline{\rho}_G^+ &= \frac{z_a e^2 \pi \beta}{\alpha_{at}} \sum_i \rho_0^+ \left[\int_0^{R_c} dS S^2 e^{-\beta S} \int_0^{\pi} d\theta \sin\theta e^{-\gamma + f(S, \theta)} + \frac{2}{\beta} \int_0^{R_c} dS S e^{-\beta S} \int_0^{\pi} d\theta \sin\theta e^{-\gamma + f(S, \theta)} \right. \\ &\quad \left. + \beta \left[R_c + \frac{1}{\beta} \right] e^{-\beta R_c} \int_0^{R_c} dS S^2 \int_0^{\pi} d\theta \sin\theta e^{-\gamma + f(S, \theta)} \right], \quad (A2) \end{aligned}$$

where ρ_0^+ and γ_+ are the pre-exponent and decay constant of the charge density of the positive ion, respectively. \mathbf{r} , \mathbf{r}' , \mathbf{S} , and θ are shown in Fig. 2 and

$$f(S, \theta) = (r^2 + S^2 + 2rS \cos\theta)^{1/2}. \quad (A3)$$

After integrating Eq. (A2), we find the following result for $\overline{\rho}_G^+$ (assuming that $|\mathbf{s}| < |\mathbf{r}|$):

$$\begin{aligned} \overline{\rho}_G^+ &= \frac{1}{\alpha_{at}} \sum_i \left[f_1(R_c, \beta, \gamma_+) \rho^+(r_i) + f_2(R_c, \beta, \gamma_+) \frac{\rho^+(r_i)}{r_i} \right] \\ &= \frac{1}{\alpha_{at}} (f_1 \rho_{1G}^+ + f_2 \rho_{2G}^+) \quad (A4) \end{aligned}$$

Fourier components of ρ_{1G}^+ and ρ_{2G}^+ can be evaluated for an ionic crystal using the formulas developed in Refs. 3 and 9. Results of ρ_{1G}^+ , ρ_{2G}^+ , f_1 , and f_2 are

$$\rho_{1G}^+(z) = \frac{2\pi}{a^2} \sum_l (-1)^{l(m_1+m_2)} \{ \rho^+[(\gamma_+^2 + G^2)^{1/2} z] [1 + z(\gamma_+^2 + G^2)^{1/2}] \gamma_+ / [(\gamma_+^2 + G^2)^{3/2}] \}, \quad (A5)$$

$$\rho_{2G}^+(z) = \frac{2\pi}{a^2} \sum_l (-1)^{l(m+m)} \{ \rho^+[(\gamma_+^2 + G^2)^{1/2} z] / (\gamma_+^2 + G^2)^{1/2} \}, \quad (A6)$$

where $\rho^+[(\gamma_+^2 + G^2)z] = \rho_0^+ \exp[-(\gamma_+^2 + G^2)^{1/2} z]$, $l=1$ is the first layer, $l=2$ is the second layer, and

$$f_1(R_c, \beta, \gamma_i) = \frac{z_a e^2 \pi \beta}{\gamma_i} \left\{ - \left[1 + \beta \left[R_c + \frac{1}{\beta} \right] e^{-\beta R_c} \right] \left\{ e^{-(\beta - \gamma_i) R_c} \left[\frac{R_c}{\beta - \gamma_i} + \frac{1}{(\beta - \gamma_i)^2} \right] - \frac{1}{(\beta - \gamma_i)^2} \right. \right. \right. \\ \left. \left. - e^{-(\beta + \gamma_i) R_c} \left[\frac{R_c}{\beta + \gamma_i} + \frac{1}{(\beta + \gamma_i)^2} \right] + \frac{1}{(\beta + \gamma_i)^2} \right\} \right. \\ \left. - \frac{2}{\beta} \left[\frac{1}{\beta - \gamma_i} e^{-(\beta - \gamma_i) R_c} - \frac{1}{\beta - \gamma_i} - \frac{1}{\beta + \gamma_i} e^{-(\beta + \gamma_i) R_c} + \frac{1}{\beta + \gamma_i} \right] \right\}, \quad (\text{A7})$$

$$f_2(R_c, \beta, \gamma_i) = \frac{z_a e^2 \pi \beta}{\gamma_i^2} \left\{ - \left[1 + \beta \left[R_c + \frac{1}{\beta} \right] e^{-\beta R_c} \right] \left\{ e^{-(\beta - \gamma_i) R_c} \left[\frac{R_c}{\beta - \gamma_i} + \frac{1}{(\beta - \gamma_i)^2} \right] - \frac{1}{(\beta - \gamma_i)^2} \right. \right. \\ \left. - e^{-(\beta + \gamma_i) R_c} \left[\frac{R_c}{\beta + \gamma_i} + \frac{1}{(\beta + \gamma_i)^2} \right] + \frac{1}{(\beta + \gamma_i)^2} \right. \\ \left. - \gamma_i e^{-(\beta - \gamma_i) R_c} \left[\frac{R_c^2}{\beta - \gamma_i} + \frac{2R_c}{(\beta - \gamma_i)^2} + \frac{2}{(\beta - \gamma_i)^3} \right] + \frac{2\gamma_i}{(\beta - \gamma_i)^3} \right. \\ \left. + \gamma_i e^{-(\beta + \gamma_i) R_c} \left[\frac{R_c^2}{\beta + \gamma_i} + \frac{2R_c}{(\beta + \gamma_i)^2} + \frac{2}{(\beta + \gamma_i)^3} \right] - \frac{2\gamma_i}{(\beta - \gamma_i)^3} \right\} \\ - \frac{2}{\beta} \left[\frac{1}{(\beta - \gamma_i)} e^{-(\beta - \gamma_i) R_c} - \frac{1}{\beta - \gamma_i} - \frac{1}{\beta + \gamma_i} e^{-(\beta + \gamma_i) R_c} \right. \\ \left. + \frac{1}{\beta + \gamma_i} - \gamma_i e^{-(\beta - \gamma_i) R_c} \left[\frac{R_c}{\beta - \gamma_i} + \frac{1}{(\beta - \gamma_i)^2} \right] \right. \\ \left. + \frac{\gamma_i}{(\beta - \gamma_i)^2} + \gamma_i e^{-(\beta + \gamma_i) R_c} \left[\frac{R_c}{\beta + \gamma_i} + \frac{1}{(\beta + \gamma_i)^2} \right] - \frac{\gamma_i}{(\beta + \gamma_i)^2} \right] \right\}. \quad (\text{A8})$$

By the same procedure we can find $\overline{\rho_G^-}$ if we change all the + subscript and superscript signs into - signs.

-
- ¹G. Vidali, M. W. Cole, and J. R. Klein, *Phys. Rev. B* **28**, 3064 (1983); G. Vidali, S. Chung, and M. W. Cole (unpublished).
²L. Bruch, *Surf. Sci.* **125**, 194 (1983); I. P. Batra, *ibid.* **148**, 1 (1984); M. W. Cole, F. Toigo, and E. Tosatti, *Surf. Sci.* **125** (1983); *Phase Transitions in Surface Films*, edited by J. G. Dash and J. Ruvalds (Plenum, New York).
³V. Celli, D. Eichenauer, A. Kaufhold, and J. P. Toennies, *J. Chem. Phys.* **83**, 2504 (1985); D. Eichenauer and J. P. Toennies, *Surf. Sci.* **197**, 267 (1988).
⁴(a) J. M. Hutson and P. W. Fowler, *Surf. Sci.* **173**, 337 (1986); (b) F. O. Goodman, and M. C. Vargar, *ibid.* **176**, 619 (1986).
⁵H. Hoinkes, *Rev. Mod. Phys.* **52**, 933 (1980) and references cited therein.
⁶F. Toigo and M. W. Cole, *Phys. Rev. B* **32**, 6989 (1985).
⁷M. Karimi and G. Vidali, *Phys. Rev. B* **38**, 7759 (1988); **36**, 7576 (1987).
⁸M. Karimi and G. Vidali, in *Diffusion at Interfaces: Microscopic Concepts*, Vol. 12 of *Springer Series in Surface Science*, edited by H. J. Kreuzer, J. J. Weimer, and M. Grunze (Springer, New York, 1988), p. 43.
⁹A. Frigo, F. Toigo, M. W. Cole, and F. O. Goodman, *Phys. Rev. B* **33**, 4184 (1986); E. Carlos and M. W. Cole, *Surf. Sci.* **91**, 339 (1980).
¹⁰J. Terrsoff, M. J. Cardillo, and D. R. Hamann, *Phys. Rev. B* **32**, 5044 (1985).
¹¹J. K. Nørskov, *Phys. Rev. B* **26**, 2875 (1982); N. D. Lang and J. K. Nørskov, *ibid.* **27**, 4612 (1983).
¹²M. Manninen, J. K. Nørskov, M. J. Puska, and C. Umrigar, *Phys. Rev. B* **29**, 2314 (1984).
¹³M. Karikorpi, M. Manninen, and C. Umrigar, *Surf. Sci.* **169**, 299 (1986).
¹⁴C. Schwartz, *J. Chem. Phys.* **83**, 437 (1985).
¹⁵J. R. Klein, L. W. Bruch, and M. W. Cole, *Surf. Sci.* **173**, 555 (1986).
¹⁶S. Rauber, J. R. Klein, M. W. Cole, and L. W. Bruch, *Surf. Sci.* **123**, 173 (1982).
¹⁷G. Vidali and M. W. Cole, *Surf. Sci.* **110**, 10 (1981).
¹⁸S. Chung and M. W. Cole, *Surf. Sci.* **145**, 269 (1984).
¹⁹E. Semerád, P. Seqward-Base, and E. M. Horl, *Surf. Sci.* **189/190**, 975 (1987).
²⁰G. Boato, P. Cantini, and L. Mattera, *Surf. Sci.* **55**, 141 (1976).
²¹P. Cantini and E. Cevasco, *Surf. Sci.* **148**, 37 (1984).
²²G. Boato, P. Cantini, and L. Mattera, *Jpn. J. Appl. Phys.* (Suppl. 2), Pt. 2 (1974).
²³G. Vidali, C. W. Hutchings, and M. Karimi, *Surf. Sci.* **202**, L595 (1988).
²⁴D. E. Vilches (private communication).
²⁵G. Derry, D. Wesner, S. V. Krishnaswamy, and D. R. Frankl,

- Surf. Sci. **74**, 245 (1978).
- ²⁶W. J. Leung, J. Z. Larese, and D. R. Frankl, Surf. Sci. **136**, 649 (1984); **143**, L398 (1984).
- ²⁷S. Sullivan, A. D. Migone, and O. E. Vilches, Surf. Sci. **162**, 461 (1985); M. Mahgerefteh, D. R. Jung, and D. R. Frankl (unpublished).
- ²⁸G. Brusdeylins, R. B. Doak, J. G. Skofronick, and J. P. Toennies, Surf. Sci. **128**, 191 (1983).
- ²⁹G. Vidali, M. W. Cole, J. R. Klein, Phys. Rev. B **28**, 3064 (1983).
- ³⁰M. W. Cole and F. Toigo, Phys. Rev. B **31**, 727 (1985).